

Polymer Imprint Lithography with Molecular-Scale Resolution

Feng Hua, Yugang Sun, Anshu Gaur, Matthew A. Meitl, Lise Bilhaut, Lolita Rotkina, Jingfeng Wang, Phil Geil, Moonsub Shim, and John A. Rogers*

Department of Materials Science and Engineering, Department of Chemistry, Beckman Institute and Seitz Materials Research Laboratory, University of Illinois at Urbana/Champaign, Urbana, Illinois 61801

Anne Shim*

Dow Corning Corporation, Midland, Michigan 48686

Received October 5, 2004; Revised Manuscript Received October 21, 2004

ABSTRACT

We show that small diameter, single-walled carbon nanotubes can serve as templates for performing polymer imprint lithography with feature sizes as small as 2 nm – comparable to the size of an individual molecule. The angstrom level uniformity in the critical dimensions of the features provided by this unusual type of template provides a unique ability to investigate systematically the resolution of imprint lithography at this molecular scale. Collective results of experiments with several polymer formulations for the molds and the molded materials suggest that the density of cross-links is an important molecular parameter that influences the ultimate resolution in this process. Optimized materials enable reliable, repetitive patterning in this single nanometer range.

New techniques for fabricating structures with nanometer dimensions^{1–3} are critically important to advances in nanoscience and technology. These methods may also play future roles in the semiconductor industry as replacements for projection mode photolithography, whose practical limits make it impossible to reach the resolution (<45 nm features) requirements for devices that are expected in 2010.⁴ Among the several next generation lithography (NGL) methods that are being explored for this purpose, those that use molds to imprint features into thin polymer films have attracted considerable attention.^{1–3,5,6} Although the well-defined optical physics associated with photolithographic techniques allows their resolution limits to be specified accurately, those of NGLs based on nanoimprinting are much more difficult to determine. The uncertain polymer physics that governs the molding process and the absence of a reliable means to evaluate the resolution at sub-5 nm length scales present significant challenges.

Resolution limits of nanoimprinting techniques are most effectively evaluated using molds that present arrays of relief structures with lateral and vertical dimensions that vary continuously from 5 nm to below 1 nm. It is extremely difficult or impossible, however, to fabricate molds of this type using conventional means, such as electron beam lithography, due to limits in resolution and patterning nonuniformities at

this scale. Molds formed by the cleaved and etched edges of substrates with multilayer stacks deposited by molecular beam epitaxy have some limited utility at the 10 nm scale, but they cover only small areas, they offer a limited range of geometries, and they are difficult to use and characterize.^{7,8} Here we show that it is possible to use high quality submonolayers of small diameter SWNTs as templates from which useful nanomolds can be constructed. The cylindrical cross sections and high aspect ratios of the tubes, the atomic scale uniformity of their dimensions over lengths of many microns, their chemical inertness, and the ability to grow or deposit them in large quantities over large areas on a range of substrates are key features for this unusual application of SWNTs. Methane-based chemical vapor deposition^{9,10} using a relatively high concentration of ferritin catalysts yields SWNTs with diameters between 0.5 and 5 nm and a coverage of 1–10 tubes/ μm^2 on SiO₂/Si wafers. The continuous range of diameters of these tubes and their relatively high, but submonolayer, coverage make them ideal for evaluating resolution limits. The cylindrical geometry of the SWNTs allows their dimensions to be characterized simply by atomic force microscope (AFM) measurements of their heights.

The work presented here uses the SWNTs to determine limits in the sizes of features that can be generated by a widely used ‘soft’ imprinting lithographic process.³ The resolution of this approach was recently examined using molds with nanometer depths of relief but with lateral dimensions

* Corresponding authors. E-mail: jrogers@uiuc.edu; anne.shim@dowcorning.com.

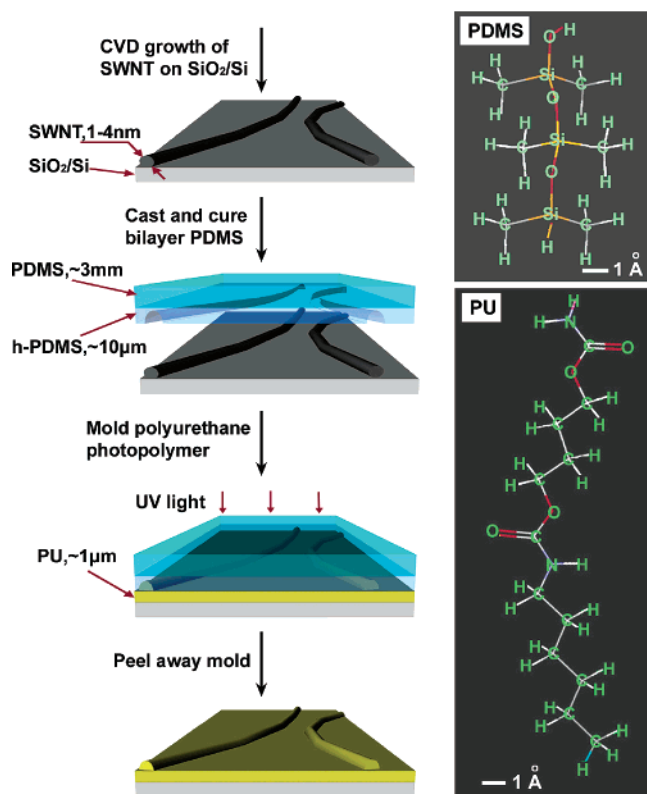


Figure 1. Steps for polymer imprint lithography with nanometer resolution. Casting and curing PDMS against a collection of SWNTs (diameters between 1 and 5 nm) generates a transparent mold with features of relief in the geometry of the SWNTs. Contacting such a mold with a prepolymer to PU and then cross-linking this prepolymer by exposing it to ultraviolet light generates a replica of the relief structure. The frames on the right illustrate several repeat units of the PDMS and PU. Two important length scales are (i) the average distance between cross-links, which is 1–2 nm for these materials, and (ii) the typical bond lengths, which are in the range of 0.1–0.2 nm.

of several microns.¹¹ The important question of limits in lateral (and vertical) resolution can be answered by using SWNT/SiO₂/Si substrates as ‘masters’ against which liquid prepolymers are cast and cured to form ‘soft’ elastomeric molds. Figure 1 illustrates the materials and fabrication steps. This procedure generates molds with true nanoscale relief structures, defined by the geometry of the SWNTs. Its success relies on (i) van der Waals adhesion forces that bind the SWNTs to the substrate with sufficient strength to prevent their removal when the cured polymer mold is peeled away, and (ii) the complete absence of polymeric residue on large regions of the SWNT masters after the fabrication process. Careful AFM measurements on the masters before and after fabricating molds verify these two important aspects. A relatively high modulus (~10 MPa) elastomer based on poly-(dimethylsiloxane) (h-PDMS) provides the surface layer for the molds. In the casting and curing process, a platinum catalyst induces the addition of SiH bonds across the vinyl groups in the prepolymer to the h-PDMS, forming SiCH₂–CH₂–Si linkages. The multiple reaction sites on both the base and cross-linking oligomers allow for 3D cross-linking, which prohibits relative movement among bonded atoms. The low viscosity (~1000 cP at room temperature) of the

prepolymer and the conformability of the silicone backbone make this material well designed for replicating fine features. Because it is brittle, a physically tough low modulus PDMS (s-PDMS) backing layer is used to make the mold easy to handle.^{12,13} For the extremely high resolution features of interest here, there are at least two important length scales: (i) the average distance between cross-links, which is approximately ~1 nm for the h-PDMS, and (ii) the chemical bond lengths, which are in the range of 0.2 nm.

A low viscosity (130 cP at room temperature) photocurable polyurethane (PU) spin cast as a thin film on a silicon wafer provides a material for imprinting. The PU formulation includes a prepolymer, a chain extender, a catalyst, and an adhesion promoter. Lightly pressing a PDMS mold against this layer causes the liquid PU prepolymer to flow and conform to the relief features on the PDMS. Passing light through the transparent mold causes the PU to undergo chain extension and cross-linking to yield a set PU with Shore D hardness of 60. Direct AFM characterization of the surface of the PU reveals, with atomic scale precision, the vertical dimensions of the imprinted relief. Figure 2 shows AFM images of a SWNT master and corresponding regions of three different PU structures imprinted with a single mold derived from this master. The unique structure of the SWNT masters allows easy direct comparisons of this type. Qualitatively, the data show that the fabrication process accurately reproduces the nanoscale features associated with the SWNTs, even for multiple imprinting cycles: the Y-shaped SWNT junction as well as the smaller tube fragments on the master are all visible in each PU sample. Line scans collected from lower left branch of the ‘Y’ structure (Figure 2 insets) show that the imprinted relief features have heights that are similar (and often identical, depending on position) to those on the master. Some of the apparent distortions in the cross-sectional shapes of these features can be attributed to AFM artifacts associated with the roughness on the surface of the molded PU. This roughness has a root-mean-squared amplitude (evaluated by AFM) of 0.37 nm for Replica 1, and 0.4 nm for Replica 2 and Replica 3. The maximum peak-to-valley height change associated with this roughness is in the range of ~1.5 nm.

Images obtained by AFM only reveal accurately the heights of the relief features. Transmission electron microscopy (TEM) can determine their widths. Poly(acrylic acid) (PAA), rather than PU, was imprinted for this purpose since PAA is a well-established polymer for TEM analysis.¹⁴ Figure 3a shows an AFM image of a PAA layer imprinted with the same PDMS mold used for the results of Figure 2, evaluated in the same region. The replication fidelity, heights of features, surface roughness, and other properties are similar to those observed in PU. Depositing (at 30 degrees to the surface of the PAA) Pt/C (to provide contrast in the TEM) and then C (at normal incidence, to provide structural support for the Pt) on the imprinted PAA and then dissolving the PAA with water generates a Pt/C membrane replica of the relief structure.^{15,16} For comparison, a similar Pt/C replica was prepared from a SWNT master by etching away the SiO₂ layer (with 2% HF in H₂O) to lift off the replica. Figure 3

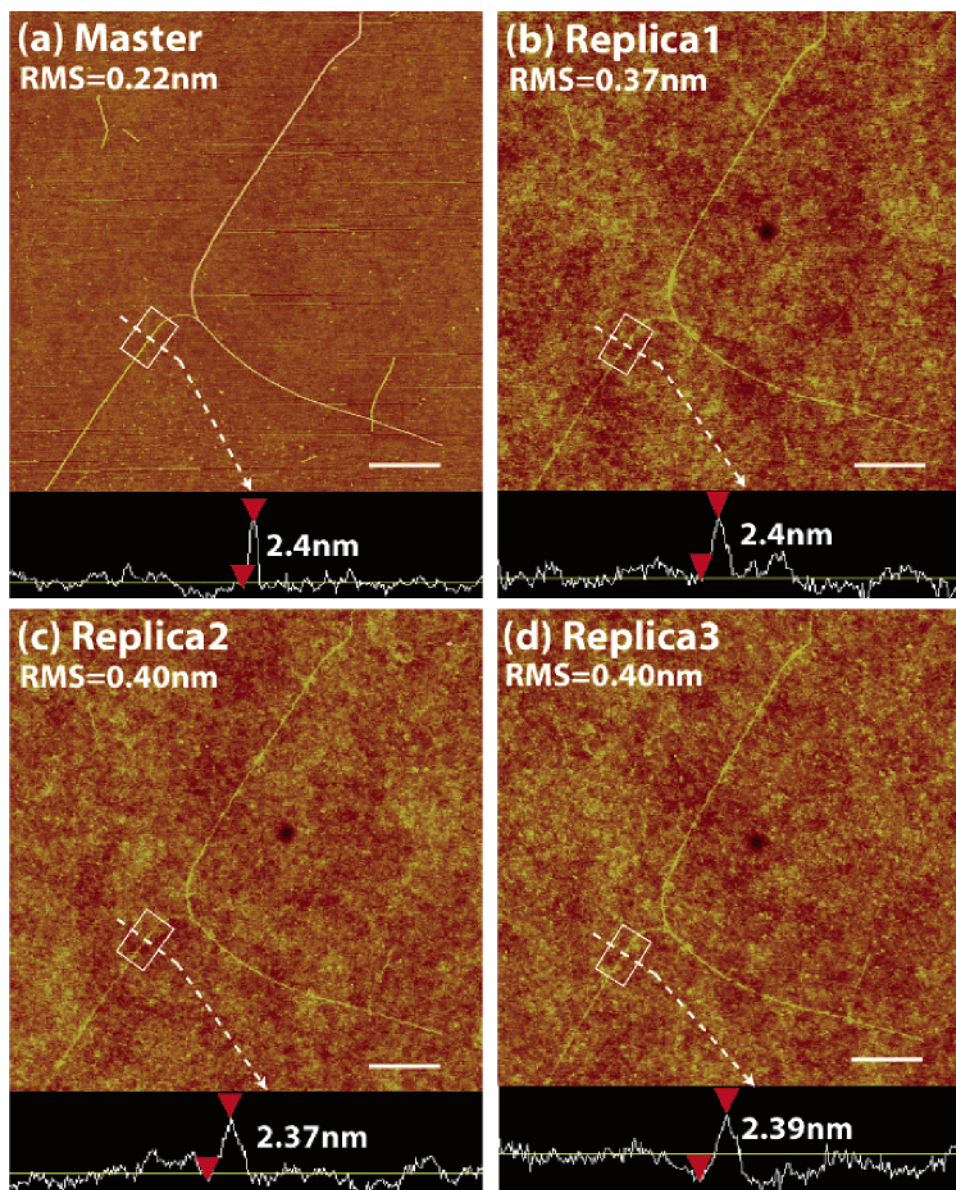


Figure 2. AFM images of a SWNT master (a) and three separate polymer nanostructures formed by imprinting using a single mold derived from this master (b–d). The scale bars are $1\ \mu\text{m}$. The images, which were collected from the same regions of each sample, show the ability to replicate accurately the nanometer scale features associated with the SWNTs. The line cuts in the insets at the bottoms of these images indicate that the imprinted polymers can, in certain regions, reproduce fully the relief heights associated with the SWNTs.

presents TEM images of both types of replicas. The dark and bright stripes along the tube features represent regions of metal build-up and shadows, respectively. The separation between the darkest and brightest regions approximately defines the width of the feature. We measured the separation by analyzing line scans of the images averaged over straight lengths (50 nm) of the relief features of interest. The profiles determined in this way from the imprinted PAA and SWNT masters most typically exhibit similar shapes. See insets to Figures 3b and 3c, which show results from different regions of a master and imprinted sample. For both samples, we observed a range of widths, between $\sim 3\ \text{nm}$ to $\sim 10\ \text{nm}$. (Widths below 3 nm were difficult to determine due, at least in part, to the apparent grain size ($\sim 1\ \text{nm}$) of the Pt/C.) The TEM data are consistent with imprinted polymer structures that have dimensions and cross-sectional shapes similar to

those on the master. In particular, the results, taken together with the AFM measurements, suggest that the heights of the imprinted features provide an approximate measure of their widths, for the cases presented here. This situation might be expected, but not guaranteed, based on the cylindrical geometry of the SWNTs.

From the AFM and TEM images, it is clear that SWNTs with diameters larger than 2.5 nm on the master appear reliably as continuous replicated features in the imprinted polymers. The heights of these features vary, however, along their lengths from a maximum that is roughly equal to the height of the SWNTs on the master to a minimum that is comparable to this height reduced by a value that is comparable to the peak-to-valley surface roughness. We believe that this roughness plays a role in, and is indicative of, the polymer physics that limits the resolution. It contributes to

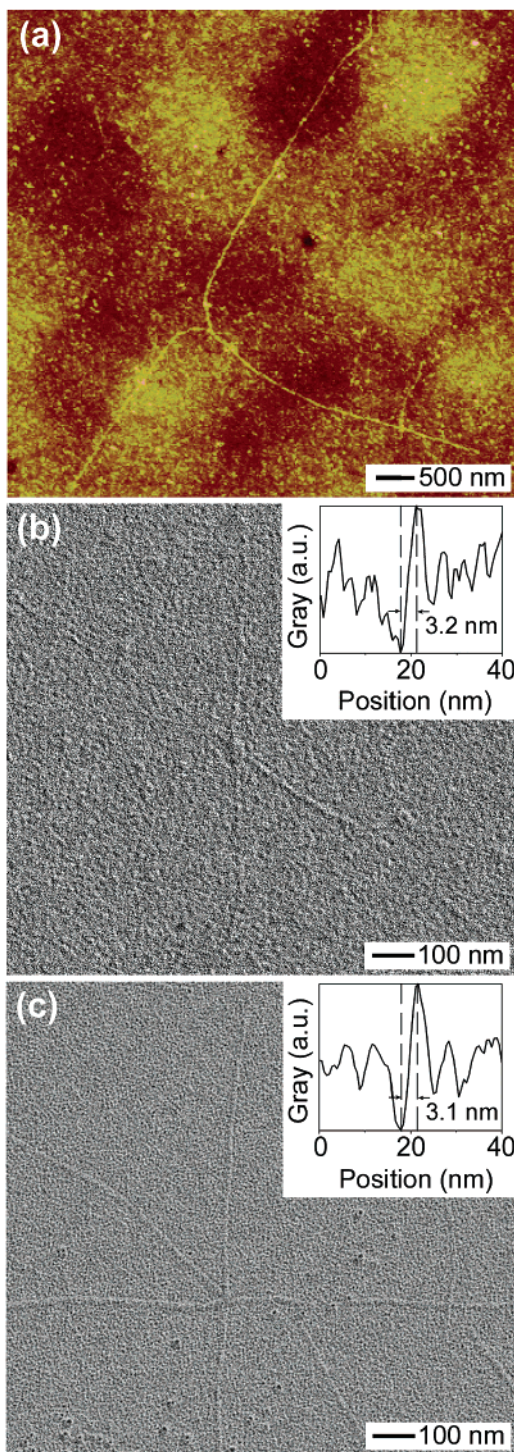


Figure 3. AFM and TEM analyses of lateral dimensions in nanoscale features formed by polymer imprint lithography. (a) AFM image of a layer of PAA imprinted with a mold derived from a SWNT master. (b,c) TEM images of Pt/C replicas formed by angled evaporation onto relief features in PAA fabricated with a similar mold and onto a SWNT master, respectively. Line cuts of the image intensity (insets), averaged along the straight lengths of features related to individual tubes, show that different structures with similar dimensions in the PAA replica and SWNT master have similar profiles.

the occurrence of breaks, or apparently missing sections, that begin to appear in AFM images of relief features associated with SWNT diameters < 2 nm. For 1–2 nm diameter

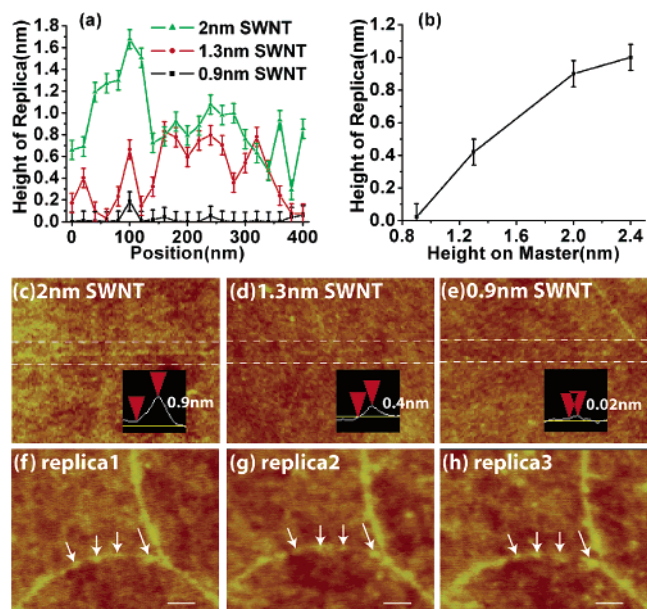


Figure 4. (a) Heights of features imprinted in polyurethane that are associated with individual SWNTs with diameters of 2, 1.3, and 0.9 nm, plotted as a function of position along these structures. (b) Length averaged height of imprinted features as a function of the SWNT diameter. (c–e) AFM images of imprinted features (within the parallel dashed lines) associated with SWNTs that have diameters of 2, 1.3, and 0.9 nm, respectively. (f–h) AFM images of relief features in three separate polymer layers imprinted using a single mold. The arrows highlight defects that appear in each of the samples. The scale bars are 100 nm.

SWNTs, these breaks represent a substantial fraction of the overall length of the imprinted structures. Below 1 nm, only small fractions of the replicated structures are visible. See Figure 4a. Even at the ~ 1 nm scale, however, it is still possible to identify the replicated relief by averaging AFM line cuts collected along the length of a feature (whose location is inferred from the positions of the SWNT on the master), as illustrated in Figure 4b. We can conclude, then, that the imprinting procedure studied here offers reliable replication capability for features with horizontal and vertical dimensions greater than 2 nm, partial capability for features between 1 and 2 nm, and little to no capability for features below 1 nm. This behavior can be summarized by plotting the position averaged relief height as a function of SWNT diameter, as illustrated in Figure 4a–e.

The ultimate resolution is correlated to the ability of the prepolymer (PDMS, PU or PAA) to conform to the surface (master or PDMS) and the ability of the polymers (PDMS, PU, or PAA) to retain the molded shape. Three pieces of data suggest that the PDMS molds limit the resolution. First, breaks (Figure 4f–h) in the molded relief features typically occur at the same positions in multiple molding cycles. Second, imprinted structures in dissimilar polymers (i.e., PU and PAA) have similar surface roughness and relief height distributions. Third, PU molded against a bare fluorinated SiO_2/Si wafer produces a surface roughness (0.19 nm) that is smaller than that generated with flat PDMS molds derived from these same wafers. Although it is difficult to assign the observed roughness and resolution limits to particular

Table 1. Average Molecular Weight between Crosslinks (M_c), Distance between Crosslinks (D), Surface Roughness, and Resolution Limits Obtained with Molds Made of PDMS with Three Different Cross-Link Densities

	theoretical cross-link distance (D) (nm)	theoretical M_c (g/mol)	experimental M_c (g/mol)	rms roughness (nm)	peak-to-valley roughness (nm)	resolution limit (nm)
h-PDMS	1.28	360	380	0.37	1.7	~2
h1-PDMS	1.6	550	540	0.54	3.1	~3
s-PDMS	2.7	1239	890	0.54	3.2	~3.5

molecular features of the PDMS, the density of cross-links is likely to be a critical parameter. To examine this possibility, we compared the performance of three PDMS materials with different cross-link densities. The average molecular weight between cross-links (M_c) and distance between cross-links (D) were determined by swelling samples in toluene and applying Flory–Huggins theory and an approach developed by Fetters et al., respectively.¹⁷ Table 1 summarizes the M_c and D values and experimental resolution limits and roughness parameters for h-PDMS, a low cross-link density version of this material (h1-PDMS), and a commercially available low modulus PDMS (s-PDMS), which has a much different molecular structure than h-PDMS or h1-PDMS. These three materials exhibit a qualitative correlation between resolution and cross-link density. They also show that the resolution and roughness are related; both are influenced by the conformability of the polymer chains and the ability of the cross-linked polymer to retain the molded shape. Attempts to improve the resolution by increasing the number of cross-links in the h-PDMS failed due to a tendency of the resulting material to stick to the SWNT ‘masters’. This result highlights the need for the molds to possess many different properties for effective use in these applications.

In summary, the results presented here illustrate a new and simple method for evaluating the resolution limits of lithographic techniques based on imprinting of polymers. When implemented with optimized polymers, this type of approach can achieve resolution approaching the single nanometer range. This performance is several times better than that described for any other method that can pattern large areas in a parallel fashion. It is of particular note that replication at the 1 nm scale involves features with dimensions that are only a few times larger than the length of an individual chemical bond in the polymer. This bonding distance may represent an ultimate limit in the resolution. The polymer science and chemistry in this regime are of considerable fundamental interest. The technology implications are significant to many fields, from semiconductor device manufacturing (where registration, residual layer thickness, etch back, and other issues that are not studied here are also very important) to emerging areas of nanobiotechnology, nanofluidics, and chemistry where the ability to mold structures with molecular dimensions might open up new pathways to molecular recognition, drug discovery, catalysis, and molecule specific chem/biosensing. These

areas, as well as relationships between the surface lithography described here, and work in unpatterned, bulk molecular templating, which is often referred to as molecular imprinting,^{18–20} represent promising directions for future work.

Acknowledgment. This work was supported by grants from Dow Corning Corporation. We thank professor J. Zuo for the helpful discussion on TEM measurement. AFM (or/and any other techniques) was carried out in the Center for Microanalysis of Materials, University of Illinois, which is partially supported by DoE (DEFG02-91-ER45439).

Supporting Information Available: The process of the nanomolding and preparation of the TEM sample. This material is available free of charge via the Internet at <http://pubs.acs.org>.

References

- (1) Kumar, A.; Whitesides, G. M. *Appl. Phys. Lett.* **1993**, *63*, 2002–2004.
- (2) Kim, E.; Xia, Y.; Zhao, X. M.; Whitesides, G. M. *Adv. Mater.* **1997**, *9*, 651–654.
- (3) Xia, Y.; McClelland, J. J.; Gupta, R.; Qin, D.; Zhao, X.-M.; Sohn, L. L.; Celotta, R. and Whitesides, G. M. *Adv. Mater.* **1997**, *9*, 147–149.
- (4) *International Technology Roadmap for Semiconductors*; 2003 edition.
- (5) Chou, S. Y.; Keimel, C.; Gu, J. *Nature* **2002**, *417*, 835–837.
- (6) Colburn, M.; Grot, A.; Amistoso, M.; Choi, B. J.; Bailey, T.; Ekerdt, J.; Sreenivasan, S. V.; Hollenhorst J.; Willson, C. G.; *Proc. SPIE* **2000**, *3997*, 453–457.
- (7) Melosh, N. A.; Boukai, A.; Diana, F.; Gerardot, B.; Badolato, A.; Petroff, P. M.; Heath, J. R. *Science* **2003**, *300*, 112–115.
- (8) Austin, M. D.; Ge, H.; Wu, W.; Li, M.; Yu, Z.; Wasserman, D.; Lyon, S. A.; Chou, S. Y. *Appl. Phys. Lett.* **2004**, *84*, 5299–5301.
- (9) Li, Y.; Kim, W.; Zhang, Y.; Rolandi, M.; Wang, D.; Dai, H. *J. Phys. Chem. B* **2001**, *105*, 11424–11431.
- (10) Kim, W.; Choi, H. C.; Shim, M.; Li, Y.; Wang, D.; Dai, H. *Nano Lett.* **2002**, *2*, 703–708.
- (11) Gates, B. D.; Whitesides, G. M. *J. Am. Chem. Soc.* **2003**, *125*, 14986–14987.
- (12) Schmid, H.; Michel, B. *Macromolecules* **2000**, *33*, 3042–3049.
- (13) Odom, T. W.; Christopher, J.; Wolfe, D. B.; Paul, K. E.; Whitesides, G. M. *Langmuir* **2002**, *18*, 5314–5320.
- (14) Oleary, K.; Geil, P. H. *J. Appl. Phys.* **1967**, *38*, 4169–4181.
- (15) Muller-Reichert, T.; Butt, H.-J.; Gross, H. *J. Microscopy* **1996**, *182*, 169–176.
- (16) Sogo, J.; Stasiak, A.; De Bernardin, W.; Losa, R.; Koller, T. *Electron Microscopy in Molecular Biology*; IRL Press: Oxford, 1987; pp 61–79.
- (17) Fetters, L. J.; Lohse, D. J.; Richter, D.; Witten, T. A.; Zirkel, A. *Macromolecules* **1994**, *27*, 4639–4647.
- (18) Wulff, G. *Chem. Rev.* **2002**, *102*, 1–27.
- (19) Katz, A.; Davis, M. E. *Nature* **2000**, *403*, 286–289.
- (20) Tully, D. C.; Trimble, A. R.; Fréchet, J. M. *Adv. Mater.* **2000**, *12*, 1118–1122.

NL048355U